

Atomic laser-beam finder

Kirsten Viering, David Medellin, Jianyong Mo, and Mark G. Raizen*

*Center for Nonlinear Dynamics and Department of Physics,
The University of Texas at Austin, Austin, TX 78712, USA*

[*raizen@physics.utexas.edu](mailto:raizen@physics.utexas.edu)

Abstract: We report on an experimental method to align a laser beam to a cloud of atoms trapped in a magneto-optical trap (MOT). We show how balanced lock-in detection leads to a very sensitive method to align the laser beam to the atoms in the plane perpendicular to the propagation direction. This provides a very reliable and fast way of aligning laser beams to atoms trapped in a MOT.

© 2012 Optical Society of America

OCIS codes: (020.7010) Laser trapping; (120.1880) Detection; (220.1140) Alignment.

References and links

1. S. R. Granade, M. E. Gehm, K. M. O'Hara, and J. E. Thomas, "All-optical production of a degenerate fermi gas," *Phys. Rev. Lett.* **88**, 120405 (2002)
2. K. M. O'Hara, S. L. Hemmer, M. E. Gehm, S. R. Granade, and J. E. Thomas, "Observation of a strongly interacting degenerate fermi gas of atoms," *Science* **298**, 5601 (2002)
3. R. Dumke, M. Johanning, E. Gomez, J. D. Weinstein, K. M. Jones, and P. D. Lett, "All-optical generation and photoassociative probing of sodium Bose-Einstein condensates," *New J. Phys.* **8**, 64 (2006)
4. M. D. Barrett, J. A. Sauer, and M. S. Chapman, "All-optical formation of an atomic Bose-Einstein condensate," *Phys. Rev. Lett.* **87**, 010404 (2001)
5. G. Cennini, G. Ritt, C. Geckeler, and M. Weitz, "Bose-Einstein condensation in a CO₂-laser optical dipole trap," *Appl. Phys. B: Lasers Opt.* **77**, 773 (2003)
6. G. Cennini, G. Ritt, C. Geckeler, and M. Weitz, "All-optical realization of an atom laser," *Phys. Rev. Lett.* **91**, 240408 (2003)
7. T. Weber, J. Herbig, M. Mark, H.-C. Naegerl, and R. Grimm, "Bose-Einstein condensation of cesium," *Science* **299**, 232 (2003)
8. T. Takekoshi, B. M. Patterson, and R. J. Knize, "Observation of optically trapped cold cesium molecules," *Phys. Rev. Lett.* **81**, 5105 (1998)
9. K. M. O'Hara, S. R. Granade, M. E. Gehm, T. A. Savard, S. Bali, C. Freed, and J. E. Thomas, "Ultrastable CO₂ laser trapping of lithium fermions," *Phys. Rev. Lett.* **82**, 4204 (1999)

1. Introduction

Optical evaporation of atoms trapped in a red-detuned focused laser beam has been a powerful technique to create degenerate gases. Using optical evaporation degenerate gases of alkali atoms have been created in lithium [1, 2], sodium [3], rubidium [4–6] and cesium [7]. Creating the tweezer trap using CO₂ lasers ($\lambda \approx 10 \mu\text{m}$) has been particularly interesting because of the low noise of these lasers as well as the very low scattering rate due to the large detuning. However, aligning the CO₂ laser beam to the trapped cloud of atoms remains a challenging task.

A standard technique to align an optical dipole trap beam is to image this beam at the location of the atoms directly onto a camera. This method is however not employable when working with a wavelength larger than the mid-infrared, due to the limited wavelength sensitivity of a CCD or CMOS camera and thus does not work for aligning a CO₂ laser beam. The second technique is to look for a change in the scattering rate of the atoms in the presence of the CO₂

laser beam. Any laser beam causes a change in the polarizabilities of the atoms by the AC-Stark shift, thus effectively changing the transition frequency. Therefore the scattering rate of atoms in the MOT changes, as the detuning of the MOT laser beams is varied. This technique has been used successfully in [8]. However, for lithium atoms the change in the scattering rate in the presence of the CO₂ laser is vanishingly small, because the ground ($^2S_{1/2}$) and excited ($^2P_{3/2}$) state polarizabilities are nearly equal. For a 50 W laser beam focused to a waist of 50 μm the change in transition frequency at the peak intensity of the CO₂ laser is less than 10 MHz. The overall change in scattering rate is therefore negligible and makes alignment using this technique unviable for lithium atoms. In [9] the authors therefore added an additional laser beam at a wavelength of 610 nm driving the 2p-3d transition. The scattering rate for this transition is highly sensitive to the alignment of the CO₂ laser and quick alignment using this technique could be achieved. However, this method requires an additional laser system to drive the sensitive transition and is therefore in general difficult and expensive to implement.

We report on the successful alignment of the CO₂ laser beam using balanced lock-in detection which relies on causing a change in spatial distribution of the atoms in the presence of the CO₂ laser beam. Balanced lock-in detection is required as the change in spatial distribution is too small to capture with a camera. The method described here requires only a few optics, two photodiodes and a lock-in amplifier. It is therefore easy to setup up and inexpensive as compared to using an additional laser system.

2. Experimental setup and sequence

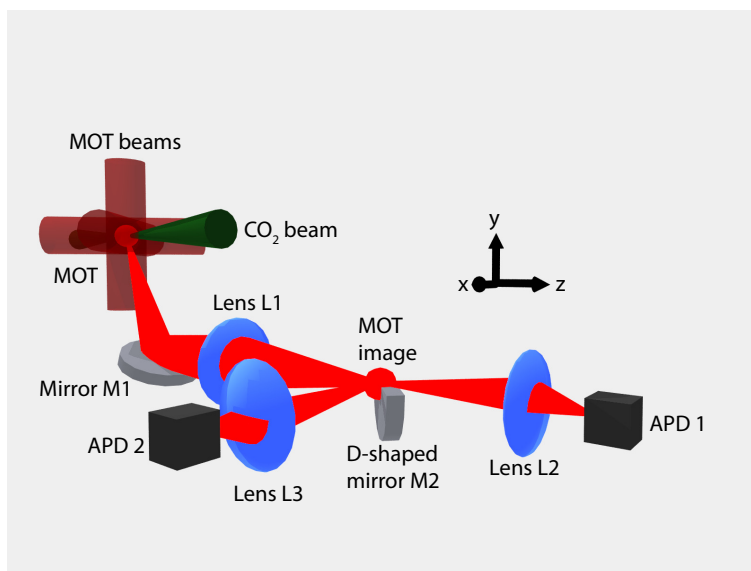


Fig. 1. Experimental setup for locating the CO₂ laser beam within the trapped cloud of MOT atoms. The three pairs of retro-reflected MOT beams excite fluorescence in the atoms of the MOT. The CO₂ beam is located in the general vicinity of the trapped cloud of atoms. The mirror M1 reflects the fluorescent light from the MOT. The lens L1 collects the fluorescent light and creates an image of the MOT. In the image plane a D-shaped mirror (M2) cuts the fluorescent signal into two halves. These are individually focused by two lenses (L2 and L3) onto two avalanche photodiodes (APD1 and APD2). The label on the coordinate system is used throughout this paper.

Figure 1 shows a schematic of the experimental setup. We load about 3×10^8 ^6Li atoms in 2 s in a MOT with a $1/e$ -radius of 3 mm (4 mm) in x (y). The MOT magnetic field gradient is 21 G/cm radially and 42 G/cm axially. The MOT beams consist of three retro-reflected beams, comprised of the two frequencies to provide cooling and repumping. The beams are detuned by 38 MHz from resonance and have an intensity of about 56 mW/cm^2 .

The CO_2 laser beam is derived from a Coherent Gem Select laser with a power of approximately 120 W and a wavelength of $10.6 \mu\text{m}$. The beam passes through an AOM and is then expanded using a 1:4 telescope. About 80 W of power is focused into the vacuum chamber using a $f = 127 \text{ mm}$ focal length plano-convex lens with a diameter of 38.1 mm. The waist at the focus is $42 \mu\text{m}$ in the horizontal and $61 \mu\text{m}$ in the vertical direction, leading to a trap depth of $\approx 730 \mu\text{K}$. The waist of the beam is measured outside the vacuum chamber using a knife-edge. In order to be able to measure the waist we insert a beamsplitter with a reflectivity of approximately 99% into the beam path to attenuate the beam power without affecting the waist at the focus. The CO_2 laser beam is aligned to the approximate location of the MOT.

As shown in Fig. 1, we collect the fluorescence light of the MOT at an angle from underneath our vacuum chamber using a mirror (M1) and a 25 mm diameter lens with focal length $f = 75.6 \text{ mm}$ (L1). This setup is determined by the optical access that we have available to collect the fluorescent light. Ideally the collection angle is maximized to capture a large number of scattered photons from the MOT atoms. Particular care is taken to reduce any scattered light from the MOT beams as much as possible in order to optimize the signal to noise levels. In the image plane of the lens L1 the signal of the MOT is split 50:50 in the vertical dimension. The light is then collected with two $f = 25 \text{ mm}$ lenses (L2 and L3) and focused onto two avalanche photodiodes (APDs). To do balanced detection the signals of the two APDs are subtracted from each other.

Figure 2 shows the measured noise spectra of (a) the electronic noise in combination with the noise caused by scattered light without atoms trapped in the MOT and (b) the noise of the system with atoms trapped in the MOT. These spectra clearly show that most of the noise is due to the scattering of photons from the atoms. Most of the noise occurs at frequencies below 2 kHz. This is explained by the timescales with which the atoms will move within the capture volume of the MOT.

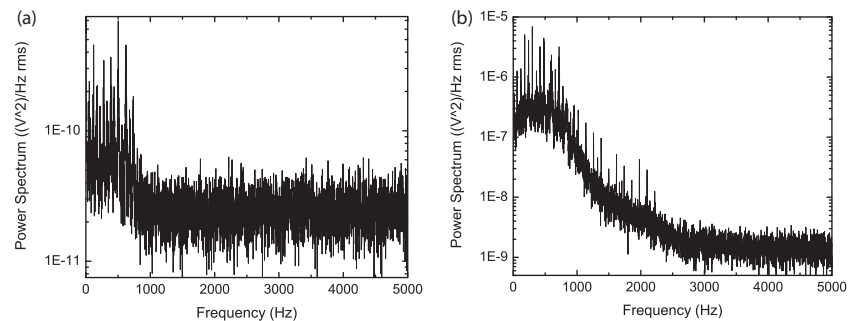


Fig. 2. (a) Electronic noise and noise caused by scattered light. (b) Noise spectrum in the presence of the MOT. In both cases the signal of the two APDs are subtracted and the difference is recorded.

At this point we can start doing the balanced lock-in detection. We pulse the CO_2 laser at a frequency f_1 by turning the AOM on and off using an RF switch. The presence of the CO_2 laser beam slightly changes the spatial distribution of the atoms within the MOT, causing a slight imbalance in the previously balanced signal from the APDs. Because this change is very small we do lock-in detection at the frequency f_1 to filter the small signal out of the large background

noise.

The ideal pulsing frequency is in principle determined by three factors: the electronic noise in the APDs and the lock-in amplifier, which we can neglect in our case, the noise caused by fluctuations in the MOT, and the timescale at which the atoms will be able to react to the presence of the CO₂ laser beam. We find that in our case the ideal pulsing frequency is around 2.4 kHz, as determined by the signal-to-noise ratio. However, qualitatively similar results can be found in the frequency range from 1.6 kHz to 2.8 kHz.

3. Results and discussion

Figure 3(a) shows a sketch of how the coordinate system at the lens used to focus the CO₂ laser into the vacuum chamber is seen at the image location of the MOT. The horizontal line indicates where the image of the MOT is split into the two separate halves. z is the propagation axis of the laser beam and passes through the center of the MOT. As an example we show how the CO₂ laser beam is moved within the cloud of atoms when the lens is moved along the y -axis (labeled (1)-(3)). The axes are defined as shown in Fig. 1.

Figure 3(b)-(d) shows the signal due to the imbalance caused by the pulsed CO₂ laser as a function of position. The stepsize is determined by the size of the MOT and the waist/Rayleigh length of the CO₂ laser. We record the signal of the lock-in amplifier at a time constant of 1 s and a sensitivity of 2 mV. We move the focus by translating the CO₂ laser focusing lens using an X-Y-Z-translation stage. As long as the laser beam hits the lens with normal incidence the translation of the lens will correspond to a 1:1 movement of the focus inside the vacuum chamber. We move the lens along one axis, leaving the other two dimensions constant. This way determining the center along the different dimensions is decoupled from the other dimensions. The numerical values of the fixed dimensions are shown in the top left corner of each graph. The error bars indicate statistical uncertainties.

Figure 3(b) shows the position dependence along the x -axis. The position of the focus along the y -axis is at $y = -0.8$ mm, 0.8 mm away from the center of the MOT. This implies that the laser beam is focused predominantly into the lower half of the MOT. As the laser focus is scanned from $x = -1.0$ mm to $x = 0$ mm we see an increase in the signal. At $x = 0$ mm the signal is maximum. Here the focus is aligned to the center of the MOT along the x -axis and therefore the laser beam affects the largest number of atoms, leading to the largest imbalance signal. If the focus is scanned further ($x > 0$ mm) the signal decreases again, as the number of affected atoms decreases. If the CO₂ laser focus was aligned to the center of the MOT along the vertical dimension ($y = 0$ mm), we would expect the imbalance caused by the laser beam to be the same in both halves of the MOT. This would mean that the average signal would be zero. In Fig. 3(c) we translate the CO₂ laser beam along the y -axis. This is the dimension along which we split the fluorescence image in the image plane of the lens L1. We can therefore expect the effect on the imbalance of the laser beam to be different than for the scan along the x -axis. At $y = 0$ mm both halves of the MOT will experience the same disturbance due to the laser beam, leading to a vanishing overall signal. As the laser focus is moved into the upper half of the MOT ($y > 0$ mm), the disturbance caused by the CO₂ laser is no longer balanced and a signal is observed. If the focus is moved past $y = 0.5$ mm the signal starts to decrease again. This is due to two reasons: the total number of atoms affected by the CO₂ laser decreases as the laser beam is moved away from the center of the MOT. In addition the effect of the disturbance of the CO₂ focus is only local. This means that even though the atomic distribution is affected by the presence of the laser beam, the overall effect is limited to only one half of the MOT and thus does not lead to an imbalance in the scattered light between the two halves. The same phenomenon is visible if the focus is moved to the lower half of the MOT ($y < 0$ mm). However, the sign of the observed signal has changed, because our system detects the difference in the

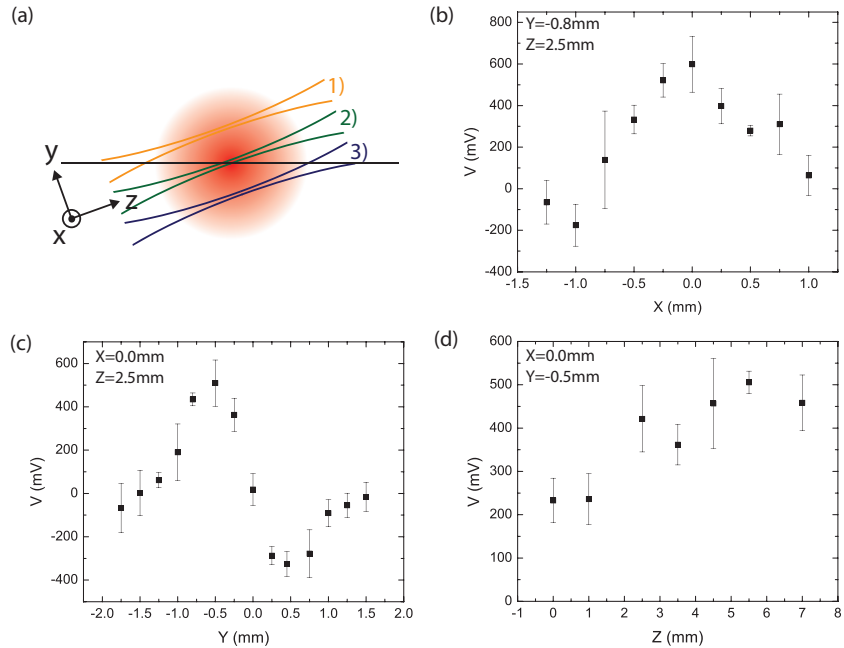


Fig. 3. (a) Geometry of the split image and laser alignment. The horizontal line symbolizes where the D-shaped mirror M2 splits the image into two halves. The two halves of the image are then detected with the two APDs. The coordinate system indicates how the coordinates at the CO₂ laser focusing lens translate at the MOT image plane. z is the propagation axis of the laser beam and passes through the center of the MOT. x (y) is the horizontal (vertical) axis at the lens position. The three focused laser beams (1-3) show the location of the CO₂ focus within the cloud for three different positions along the y -axis. The green beam (2) corresponds to the focus being aligned to the center of the MOT along the y -dimension, where the overall signal vanishes (see Fig.(c)) (b)-(d) Signal due to the imbalance caused by the pulsed CO₂ laser as a function of position. The focus of the laser beam is moved along one dimension, while the other two are held constant. (b) The focus of the laser beam is moved along the x -axis. (c) The focus of the laser beam is moved along the y -axis. (d) The focus of the laser beam is moved along the z -axis (along the beam propagation axis). Error bars indicate statistical uncertainties. The inset in the upper left corner indicates the alignment in the other two dimensions.

APD signals, not the absolute value. Figure 3(d) shows that the method we describe in this paper is not very sensitive to the alignment of the focus along the beam propagation axis, as expected from the long Rayleigh length along this dimension. The Rayleigh lengths of our CO₂ are 522 μm and 1102 μm respectively.

With the CO₂ laser pre-aligned to the general location of the MOT, a first signal can easily be found. Once a first signal is detected, a systematic scan of the focus of the CO₂ laser beam in combination with an understanding of the geometry of the setup finds the center of the MOT. First the center along the x -axis is determined by finding the maximum signal when scanning along the x -dimension, as long as $y \neq 0$ mm. Having found the center along the x -axis, the center along the y -axis is determined by scanning the y -dimension. Because the method described is insensitive to the precise location along the z -dimension, the optimization along this axis is best done by directly maximizing the number of atoms transferred into the CO₂ laser dipole trap. Using this alignment procedure we are able to align the CO₂ laser beam to the center of the MOT.

4. Conclusion

In this paper we have presented a novel technique to align a laser beam to a cloud of trapped atoms. We demonstrated that we can align the focus created by a CO₂ laser beam to the center of an atomic cloud in the plane perpendicular to the laser beam propagation. This leaves one degree of freedom (along the beam propagation axis) left to be aligned. Fortunately this dimension is the least critical due to the larger Rayleigh length of a laser beam as compared to its waist.

Acknowledgments

The authors acknowledge support from the Sid W. Richardson Foundation and the Norman Hackerman Advanced Research Program under grant number 003658-0019-2009. D.M. acknowledges support from El Consejo Nacional de Ciencia y Tecnología (CONACYT) for his graduate fellowship (206429). K.V. acknowledges support from a University of Texas Continuing Fellowship.